Int. Assoc. Sedimentol. Spec. Publ. (2009) **42**, 185–200

Molluscs as a major part of subtropical shallow-water carbonate production – an example from a Middle Miocene oolite shoal (Upper Serravallian, Austria)

MATHIAS HARZHAUSER* and WERNER E. PILLER†

*Natural History Museum Vienna, Burgring 7, A-1014 Vienna, Austria (E-mail: mathias.harzhauser@nhm-wien.ac.at)
†Institut für Erdwissenschaften, Bereich Geologie und Paläontologie, Universität Graz, Heinrichstrasse 26, A-8010 Graz, Austria

ABSTRACT

Molluscs are usually subordinate contributors to Cenozoic subtropical carbonate factories. A spectacular exception is represented by the shell-carbonate deposits from the Middle Miocene of the Vienna Basin (Austria). These strata consist of up to 81% shells and shell-hash of marine bivalves and gastropods. These locally widespread deposits fill the inlet of an Upper Serravallian (= Sarmatian regional stage) oolite shoal, forming foresets of 10-13 m height and slope angles of 20°.

Medium- to small-sized shell dunes of up to 280 cm height and shell ripples of 10 cm height and up to 190 cm length can be distinguished within the foresets. Due to amalgamation and mechanical nesting of shells, the ripples grew into the direction of the flow and were run over by subsequent ripples. The piling of shells causes stoss sides with high preservation potential within the ripples. The shells and shell-debris involved in the dune formation are interpreted to be derived from the surrounding shoal. The geometry of the foresets, dunes and ripples documents a dominant current entering a shallow lagoon framed by oolite shoals via an inlet. Based on the palaeogeographic position, these bedforms are interpreted to indicate the presence of a subaqueous flood-tidal delta marking the entrance into a shallow lagoon.

The absence of corals and corallinacean algae and a relatively reduced biotic inventory following a major extinction of marine biota in the enclosed Sarmatian Sea, allowed a few pioneer mollusc species to settle the coasts in considerable numbers. Due to the absence of the classical constituents of a shallow-water subtropical carbonate factory (i.e. a photozoan association), molluscs came to dominate carbonate production.

Keywords Oolite shoal, molluscs, flood-tidal delta, shell dunes, Miocene, Vienna Basin.

INTRODUCTION

The Middle Miocene Sarmatian stage, a regional equivalent of the Upper Serravallian (Fig. 1), coincides with the last marine phase of the European Central Paratethys Sea. Due to the sea-level low coinciding with the glacio-eustatic isotope event MSi-3 at 12.7 Ma (Abreu & Haddad, 1998), strong restrictions of the open ocean connections of the Central Paratethys occurred (Harzhauser & Piller, 2004a). This induced the development of a highly endemic marine fauna that lacks any stenohaline organisms, pointing to shifts of the water chemistry (Piller & Harzhauser, 2005). Simultaneously, changes in ecosystem complexity and food-webs occurred. Many predators preying on molluscs, such as crustaceans, carnivorous gastropods and durophagous fishes disappeared. The fully endemic development is reflected in a regional eco/biostratigraphic zonation based on molluscs and benthic foraminifera (Fig. 1).

The Lower Sarmatian in the western part of the Vienna Basin is generally dominated by fine-grained siliciclastics. Carbonates are rare, except for small bryozoans-serpulid-algal-microbial bioconstructions. During the *Ervilia* Zone, sedimentation switched from a siliciclastic dominated system to a carbonate depositional environment, characterized by more than 20 m thick Upper Sarmatian carbonate platforms with oolites and foraminiferal (nubeculariid)

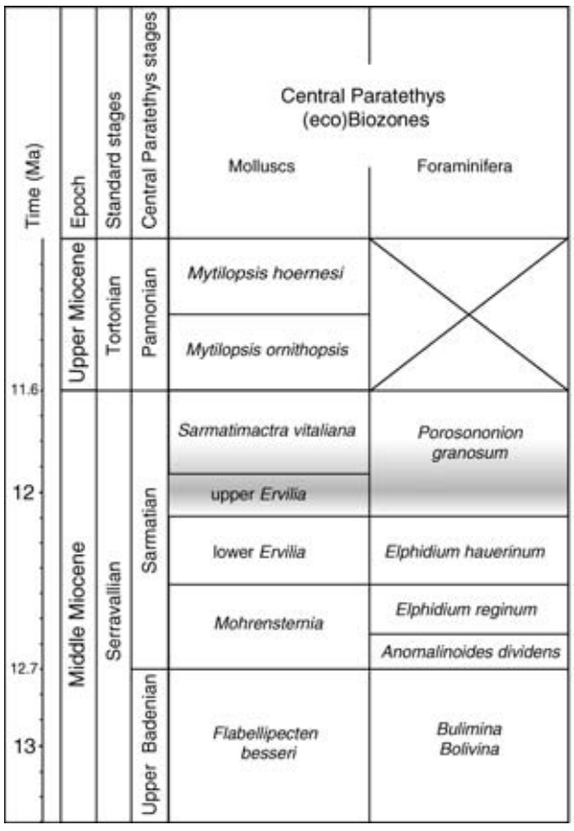

Fig. 1. Miocene chronostratigraphy of Europe. Modified after Rögl (1998) and Harzhauser and Piller (2004a), including the mollusc-based ecostratigraphic zonation of the Sarmatian. The grey-shaded area indicates the stratigraphic position of the investigated deposits.

bioconstructions. Piller & Harzhauser (2005) observed a contemporaneous increase in shell thickness of bivalves. A unique feature related with the oolite shoals are the rock-forming mollusc-shell-hash deposits at Nexing in the Vienna Basin (Lower Austria). This locality, designated as the holostratotype of the Sarmatian Stage (Papp & Steininger, 1974), is characterized by largely biogenic sediments. The sedimentological setting of the section was interpreted by Papp & Steininger (1974) as a strongly agitated shallow sublittoral zone close to the mainland. In the present study these strata are interpreted as subaqueous tidal deposits that formed along the rim of an oolite shoal. The specific environmental framework allows answers to be given concerning the important question why molluscs, characteristic of heterozoan carbonates *sensu* James (1997), can substitute the classical coralgal carbonate factory (heterozoan carbonates) in shallow-water subtropical settings.

GEOLOGICAL SETTING

The study area is situated in the northern Vienna Basin, a pull-apart basin about 200 km long surrounded by the Eastern Alps, the West Carpathians and the western part of the Pannonian Basin (1988; Fig. 2). The Sarmatian portion of the 7000 km thick Neogene basin fill attains more than 1000 m in the central Vienna Basin (Harzhauser & Piller, 2004a, b).

The deposits at the Nexing section (Fig. 2B) are part of the Miocene sediment-cover of the Mistelbach tectonic block. This tectonic unit represents a marginal block of about 60 km length and 18 km width that is separated from the deeper Vienna Basin by the Steinberg fault zone (Kröll & Wessely, 1993). The Steinberg elevation and the bordering fault zone have been the target of many geological studies during the pioneer-phase of Austrian petroleum exploration (e.g. Friedl, 1936). Generally, most of the Sarmatian succession is covered by Upper Miocene (Pannonian) fluvial and limnic deposits or by Pleistocene loess, obscuring the facies relationships of the Sarmatian. Nevertheless, age-equivalent deposits are exposed in several outcrops that have been studied during the current project (Fig. 2).

According to the regional eco/biostratigraphic zonation, the Nexing section encompasses the Upper *Ervilia* Zone and lowermost *Sarmatimactra* Zone in terms of mollusc zonation (Fig. 1), and the Lower *Porosononion granosum* Zone of the benthic foraminiferal zonation. The boundary between the Upper *Ervilia* Zone and the *Sarmatimactra vitaliana* Zone is situated at the base of Unit 3 (Fig. 3). The dating is based on the occurrence of the cardiid *Plicatiforma latisulca* (Münster) and the evolutionary levels of the gastropod *Duplicata duplicata* (Sowerby) and of the bivalves *Ervilia dissita podolica* (Eichwald), *Venerupis gregarius* (Partsch) and *Sarmatimactra eichwaldi* Laskarev (see Papp, 1956, for details).

Material and methods

The outcrop covers an area of about 0.2 km^2 (Fig. 2C). It is currently divided into an active pit in the east and an abandoned quarry in the west. The mined bioclastic sediments have been used as bird food for a long time. The quarry walls are roughly oriented WNW-ESE and SW-NE. Seven sections have been logged, providing an excellent insight into the facies architecture and the texture of the deposits. Six of these profiles are illustrated in Fig. 3. The total thickness attains about 19 m,

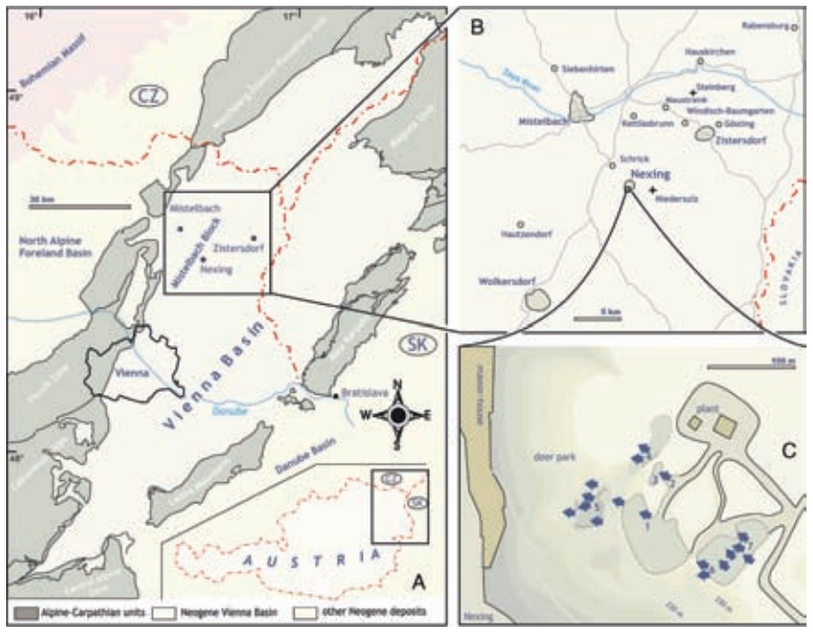

Fig. 2. Location of the study sections. (A) Regional location maps of the investigated sections on the Mistelbach block along the margin of the Vienna Basin. (B) Geographic position of the outcrop at Nexing (Austria). (C) Overview of the outcrop with the position of the investigated stratigraphic sections (Nexing 1-7). Arrows represent dip directions of the foresets. CZ = Czech Republic; SK = Slovakia.

representing a small part of the Upper Sarmatian Skalica Formation (Harzhauser & Piller, 2004a). The stratigraphic succession has been divided into four main units on the basis of lithology, sedimentary structure and biotic content (Fig. 3). Logs can be correlated laterally by a marker interval (Unit 3 in Fig. 3). A granulometric analysis has been performed for eight samples. To achieve a reliable ranking of quantitatively important mollusc species, which are the main constituents of the foresets and shell dunes (see below), five bulk samples (same numbers as granulometric samples in Fig. 3) were taken at the section covering all important lithological units. The samples were sieved through a 1 mm screen, divided into four splits, and all taxa of each split were counted. Additional data about the lateral variation and character of the Sarmatian carbonates are provided by nine well logs drilled by the OMV-AG oil company (see Harzhauser & Piller, 2004a).

RESULTS

Lithofacies units

Unit 1

The lower part of the deposits only crops out at section Nexing 1. Green silt with scattered plant debris (1.5 m thick) forms the lowermost unit. The silt bed dips 15°-16° toward the NW. Any macrofauna is missing. The scarce microfauna consist of foraminifera, such as *Porosononion granosum* and various elphidiids.

Unit 2

The silty sediment of Unit 1 is overlain by about 14 m of steeply inclined planar-bedded foresets of coarse mollusc shell-hash (Unit 2; Fig. 4A). The sediment is a bioclast-supported, polytaxic skeletal concentration (Figs 4A-B and 5A-F). The carbonate content of the sediment, such as that illustrated in Fig. 5A-D, ranges from 78-81%. This content may decrease to 60 % in poorly sorted layers with higher amounts of siliciclastics (e.g. Fig. 5E-F). Aside from the predominance of biogenic components, the poorly sorted sediment consists of medium to coarse quartz sand, associated with ooids, scattered pebbles of Cretaceous sandstone and rare reworked oolite clasts. These coquinas are very poorly sorted because the bioclasts (~2-30 mm) are generally larger than the bulk of the siliciclastic components, whilst the pebbles and oolite clasts surpass the bioclasts in size (up to 80 mm).

The thickness of the foresets ranges from 80 to 280 cm, being separated by fine to medium sand intercalations of 1-30 cm thickness. Occasionally,

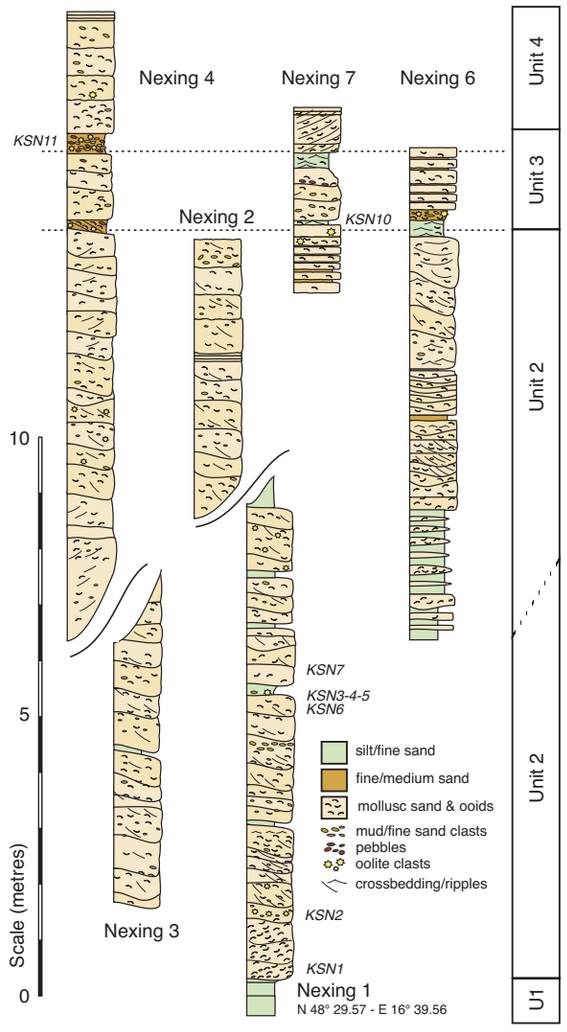

Fig. 3. Logs of the sections Nexing 1-4 and 6-7. The sandy intercalations at the base and the top of Unit 3 are used as reference levels to correlate the sections (dashed lines). KSN refers to samples mentioned in the text.

this siliciclastic intercalation is missing, and reworked lithoclasts occur in the shell bed. Lower parts of that unit, as exposed in the Nexing 1 and 3 sections, display planar bedding of more or less parallel foresets. Towards the top, exposed in sections Nexing 2, 4 and 6, the sets are divided by shallow and broad channel-like structures with thick silt to fine sand drapes of up to 40 cm thickness. The foresets dip at angles ranging from 21° to 36° in a west to NW direction. A general steepening of the foresets from base to top occurs, with angles from 21°–28° in the lower part of the unit, and 30°-36° in the upper portion. However, the dip-angles distinctly decrease in the uppermost parts of the shell-hash foresets, where values of 15-25° are measured.

Unit 3

This unit represents a marker interval allowing a lateral correlation across the outcrop area due to the marked lithological change. At section Nexing 4, it consists of a 20-180 cm thick layer of silty fine sand bearing well-rounded pebbles of Cretaceous sandstone, oolite pebbles (Fig. 6A-C) and mud to fine sand clasts of up to 5 cm diameter. Large-sized molluscs of up to 6 cm diameter (e.g. *Sarmatimactra*) are embedded within these deposits. Laterally, sections Nexing 6 and 7 show a decrease in the amount of pebbles and 10-30 cm of silt and fine sand with well-developed small-scale wave-ripples of 6-14 cm length (Fig. 6D). These ripples are overlain by 100-150 cm inclined planar-bedded mollusc shell sand with sand intercalations and frequent pebbles and reworked rhizoliths. The latter are irregular, tube-like, glossy brown calcite structures representing reworked root-horizons (Fig. 7). The dip-angle of this bed ranges from 15° to 4°. At Nexing 7, another layer of 30-50 cm of silt and fine sand with small-scale ripples follows; the dip-angle is around 4°. Again, this layer of well-sorted sediment changes within 150 m towards the NW and is replaced by fine sand with well-rounded oolite pebbles and Cretaceous sandstone pebbles at section Nexing 4 (Fig. 6C).

Unit 4

Unit 4 has a sharp lower boundary, which is overlain by a 2-3 m thick, steeply inclined, planar-bedded shell-hash. In terms of composition and sedimentary structures, deposits are similar to Unit 2, but dip-angles are lower, with values between 12° and 25°. This Miocene unit grades into various silty, sandy and gravelly layers with shell-hash, which are interpreted as reworked deposits of Pleistocene age, as supported by the relation of the deposits to the adjoining Pleistocene loess.

Sedimentary structures

Dune and related terms such as sandwave and ripple are frequently used in the literature with a broad spectrum of meanings (Allen, 1980; Boersma & Terwindt, 1981; Dalrymple, 1984; Galloway & Hobday, 1996; Leclair, 2002). *Subaqueous dune* is used herein according to Ashley (1990), who

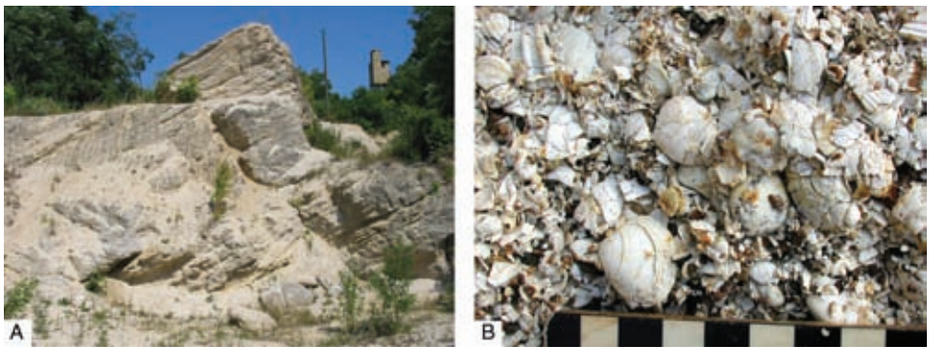

Fig. 4. Steeply inclined planar-bedded foresets of coarse mollusc shell-hash (Unit 2). (A) Lower part of the succession, representing a lateral equivalent of Nexing 1 (total height of outcrop approximately 15 m). Up to 80% of the foresets are made up of mollusc shells. The dip of the foresets is roughly toward the WNW. (B) Lower bounding of a shell ripple; viewer looks from the lee-side. Most of the shells are strongly fragmented and abraded to various degrees. The large shells are *Venerupis gregarius*. Scale bar units: 1 cm.

pointed out the preference of that term over terms such as megaripple or sandwave. Many authors, such as Allen (1980), Galloway & Hobday (1996) interpreted dunes/sandwaves as several metres long, flow-transverse bar macroforms triggered by currents of tidal origin. As the structures described herein are characterized by a composition dominated by mollusc shells, the bedform is regarded as being a shell dune. Consequently, the low-order bedforms superimposed on or constituting the structures are termed shell ripples. A closer examination of the planar-bedded foresets reveals a complex internal geometry. Three different bedform types of different hierarchical order can be defined on the basis of size and texture:

Bedform type 1

The Bedform Type 1 is a composite bedform. It comprises foresets (Fig. 4A) that range in thickness from 80 to 280 cm. When optimally preserved, single sets are separated by silt/sand-drapes of 1-30 cm thickness. These drapes became frequently eroded during the deposition of the subsequent set, but they are usually traceable as clasts in the basal part of the overlying set. The drapes consist mainly of silty fine sand with planar bedding and rare cm-scale cross bedding at the top, whilst pure clay and silt layers are very rare. In some cases, they are replaced by well-sorted, fine shell-hash.

Bedform type 2

Bedform Type 2 consists of shelly dunes, which are bundled into Bedform Type 1 (Fig. 8A). Individual shell dunes may reach a length of several metres, and more than 1 m in height, They are separated by thin drapes of fine to medium sand (sometimes replaced by shell-hash). Figure 8 illustrates a part of such a structure being composed of ripples, which represent the third bedform type. The separating layers of shell-hash and sand are well developed in Fig. 5B and D.

Bedform type 3

The shell dunes are subdivided into a smaller-scaled bedform type, termed herein *shell ripple* (Figs 5F and 11.8B). Individual ripples are up to 190 cm long and 10 cm high. Hence, the shell ripples attain heights ranging from 3.5 – 10% of the total height of the foresets. Internally, the ripples are composed of shell-hash and mollusc shells. Fossils are predominantly abraded fragments. Well-preserved valves are only a subordinate component. Shells and shell debris are associated with up to 8 cm large pebbles of well-rounded Cretaceous sandstone and oolites. Fine to coarse sand and reworked single ooids are common.

Due to cementation, only few ripples are appropriate for granulometric analysis (Fig. 9). The grain-size distributions of the measured samples display two patterns. Samples KSN3, 4, 5 and 6 show a distinct bimodal distribution with peaks at 0-1Φ and at 3-4Φ. In contrast, samples KSN1, 2 and 7 have a unimodal distribution with a peak around 0-1Φ. The sorting (method of Folk & Ward, 1957) ranges between 1.82 and 2.0 for bimodal samples and from 1.1 to 1.36 for unimodal samples, thus in

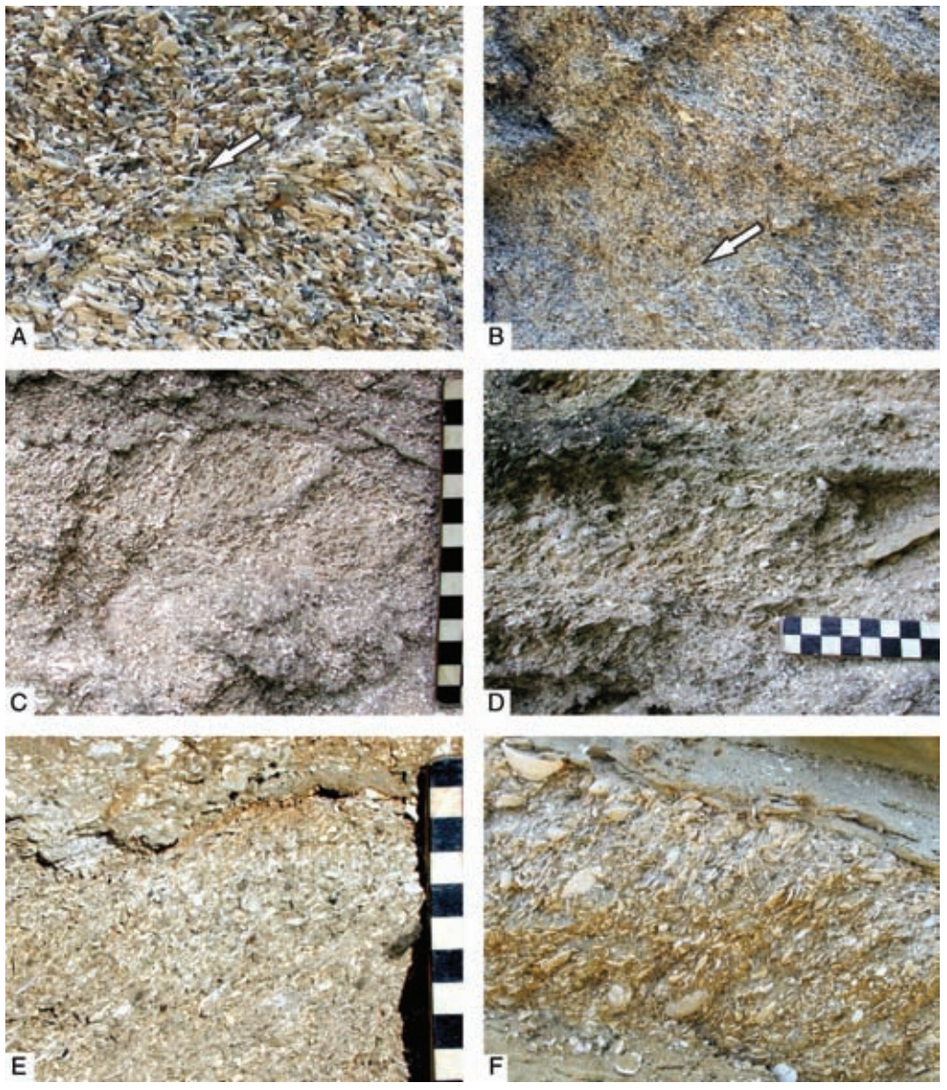

Fig. 5. Outcrop photographs of various shell ripples and shell dunes showing the eye-catching imbrication of shells. (A) Detail of two shell ripples separated by a layer of better sorted and planar-bedded shell-hash, indicated by arrow (flow from right; length of picture = 3.2 cm). (B) Distal part of a shell dune, separated from underlying and overlying dunes by poorly developed shell drapes indicated by arrow (flow from right; length of picture = 8.7 cm). (C) Shell ripple in the centre of the picture forming the crest of a shell dune. A drape of sand is well developed (flow from left). Scale bar units: 1 cm. (D) Similar situation as (C); shell ripple in the centre of the picture with drape separating two dunes. Note the pebble on the right which follows the imbrication of the shell along the stoss (flow from left). Scale bar units: 1 cm. (E) Proximal part of shell ripple showing the increasing imbrication (flow from left). Scale bar units: 1 cm. (F) Centre of an isolated shell ripple that developed within two sand drapes. Note the steep-angled imbrication and the tendency of large valves to lie with the convex side in the lee direction (flow from left; length of picture = 13 cm).

both cases representing poorly sorted sediments. The shell ripples are usually separated by densely packed, roughly planar-bedded shell-hash, but lack silt - fine sand drapes (Fig. 5A).

The elongated shell ripples display a complex internal texture: the basal layer of a shell ripple is formed by planar-bedded shell-hash and shells with admixed sand, ooids and scattered pebbles. At the leeward side of the ripple, the shells and fragments are arranged in a rather chaotic pattern but soon start to become imbricated on the stoss-side (Fig. 5F). This imbrication starts with a low-angle amalgamation of shells with a tendency for orientation of the convex sides towards the

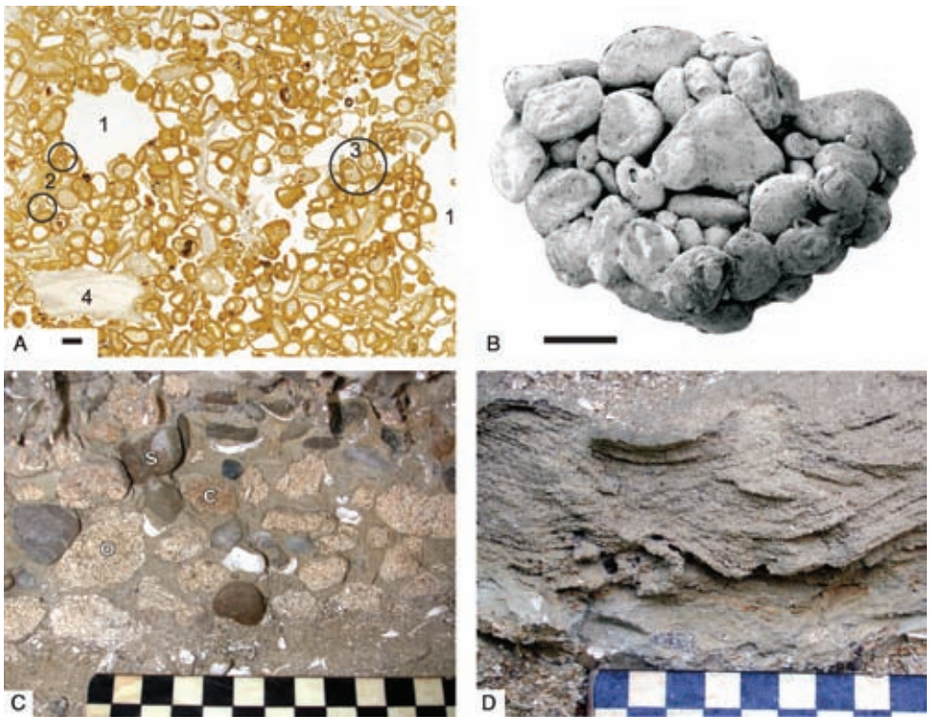

Fig. 6. Sedimentological characteristics of marker Unit 3. (A) Thin-section of an oolite pebble in Unit 3. (1) Large dissolution vugs are frequent. In addition to quartz grains and shell-hash, (2) miliolid foraminifera and (3) hydrobiid gastropods are the most abundant nuclei in the ooids. Larger bioclasts such as (4) cardiid shells lack the coatings (scale bar: 1 mm). (B) SEM photograph of an oolite clast from Unit 2; an ooid in the front bears a small-sized gastropod as a nucleus (scale bar: 1 mm). (C) Sand-supported conglomerate in the upper part of Unit 3 with well-rounded sandstone pebbles (s), carbonate concretions (c) and reworked oolites (o). Scale bar units: 1 cm. (D) Wave ripples made up of fine to medium sand in the lower part of Unit 3, close to sample KSN10. Shell-hash stringers are frequent. Scale bar units: 1 cm.

lee-direction. This "convex-side down-forward" pattern is most obvious on the bedding planes of the ripples (Fig. 4B).

The accretion of shells culminates in imbrications with steep dip-angles of up to 50–70°. This texture is best developed in the middle part of the ripple and starts to degrade towards the stoss-side due to gradual overtilting (Fig. 5E). Thus, shells and fragments tend to be arranged rather randomly or more or less parallel to the angle of the stoss.

Biota

Up to 81% of the deposits consist of skeletal grains derived almost exclusively from molluscs. Bivalves are only found with disarticulated valves. Abraded shells are typical for both bivalves and gastropods. Based on the collections of the Natural History Museum Vienna, 21 gastropod species and 11 bivalve species are recorded from the current outcrop (Table 1). In contrast to the 32 species known from museum collections, only 17 species were identified in the bulk samples (Fig. 10). A total of 1837 mollusc specimens could be identified in these five bulk samples (Fig. 10). The quantitatively most important species are the same in all standardized samples from five different shell beds. In all samples, a very small number of species contribute up to 92–98% of the biogenes. These are *Granulolabium bicinctum* (batillariid gastropod), *Venerupis gregarius* (venerid bivalve), *Obsoletiforma obsoleta vindobonensis* (cardiid bivalve), *Hydrobia frauenfeldi* (rissoid gastropod), *Sarmatimactra vitaliana* (mactrid bivalve), *Ervilia dissita podolica* (mesodesmatid bivalve), and *Cerithium rubiginosum* (cerithiid gastropod). Species-sampling curves for the splits level off nearly immediately. Thus, the sampling intensity is adequate for the documentation of all important species; even most of the rare taxa are registered.

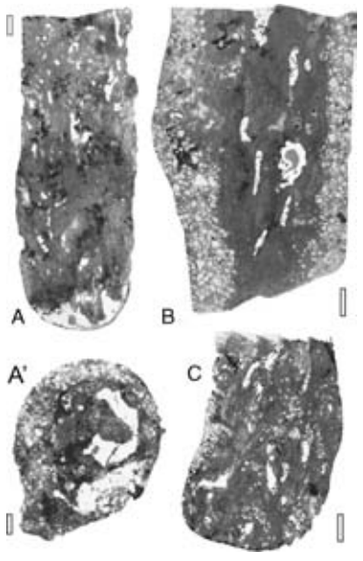

Fig. 7. Rhizoliths from Unit 3. (A-C) Tangential sections. (A') Cross-section. Note the characteristic halo of quartz sand. This decalcified zone is interpreted to result from dissolution by the acidic microhabitat surrounding the roots (scale bars: 1 mm).

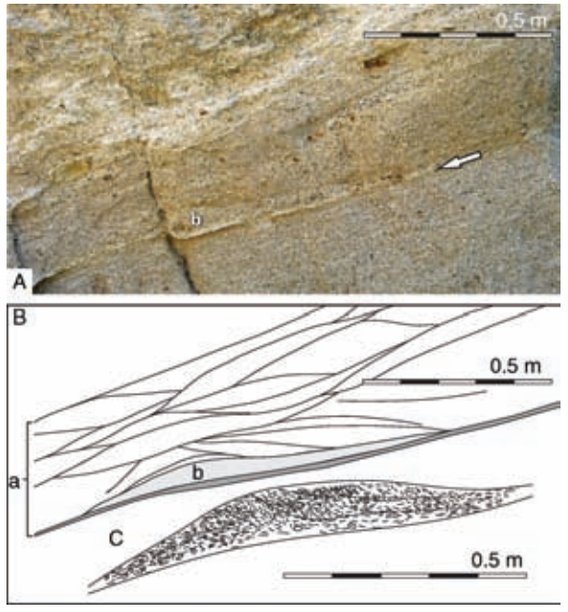

Fig. 8. Bedform Type 2 shelly dunes. (A) Outcrop photograph showing Bedform Type 2, a shell dune with mud-drape at the base (arrow). (B) Sketch illustrating the internal structure of the dune (a), formed by stacked shell ripples (b; Bedform Type 3). (C) The orientation of shells and fragments in one ripple. Steepest angles and maximum imbrication is achieved in the middle part of the ripple, overlying a basal layer of more or less planar-bedded shell hash. A further, faint, subdivision of the ripple is indicated by the dashed lines.

INTERPRETATION

Lithofacies

The high angles of the slipfaces of the foresets in Unit 2 seem to be tectonically accentuated. In fact, a back-tilting of about 15° is required if one assumes that the thin-bedded, plant-debris bearing silt of Unit 1 was originally horizontally bedded (Fig. 11). Consequently, the slope angles are around 6-15° in the lower part of Unit 2, increase to around 20° in the middle part, and decrease to angles between 10 and 20° towards the top of Unit 2. This pattern results from the gradual progradation in western and north-western directions. However, this back-tilting would cause an impossible "updipping" if applied to the wave ripple-bearing layers in Unit 3. This points to a tectonic phase prior to the formation of Unit 3, causing a 15° tilt of Units 1 and 2.

This interpretation is strongly supported by the deposition of gravel and reworked oolites at the base of Unit 3. The oolites were weakly lithified by submarine isopachous fibrous carbonate cement prior to erosion and transportation. Moreover, the frequent rhizoliths (Fig. 7), document an episode of emergence and vegetation of the area. After that phase, the last Sarmatian flooding during the *Sarmatimactra* Zone (Harzhauser & Piller 2004a) initiated the development of a second but less prominent unit of foresets. Therefore, the more or less undisturbed top of the section (Unit 4) was deposited with slope angles fully corresponding to the (back-tilted) foresets of Unit 2.

The current outcrop situation allows estimates of the length and width of the sedimentary bodies to be made. The foresets in the lower part of Unit 2 display more or less straight "crests" and planar slopes. The length of the slopes, based on outcrop observations, can be estimated to attain at least 30-40 m. Taking the calculated dip-angle of 20° into consideration, a height of about 10-13 m can be predicted for that structure. This rough estimation is corroborated by the outcrop at section Nexing 1m where the base the foresets is exposed. Consequently, the lowest dip-angles, observed at the base of the succession, correspond to very distal parts of the slipfaces, indicating early progradation.

The sedimentological interpretation of the deposits strongly relies on the general palaeogeographic framework. As shown in Fig. 12, the

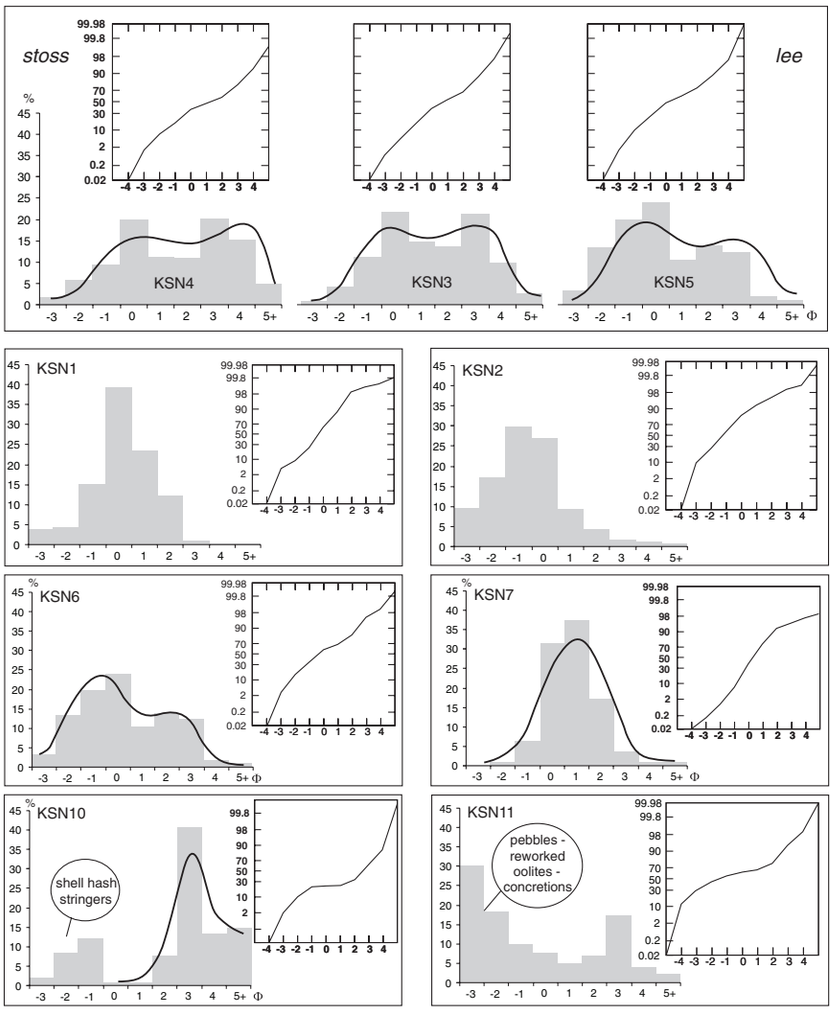

Fig. 9. Grain size distributions and cumulative probability curves of selected samples. Within the shell ripples, a bimodal grain-size distribution of samples KSN3-6 contrasts with a unimodal distribution of samples KSN1, 2 and 7. KSN10 derives from the sandy wave ripples illustrated in Fig. 6D. The coarse peak results from admixed shells. The extremely poorly sorted sample KSN11 derives from Unit 3 and yields a mixture of reworked shell dunes, oolites, fluvial pebbles and sand that formed during the renewed transgression in the latest Sarmatian (cf. Fig. 13E).

locality of Nexing is situated in a seaway or channel framed by ooid shoals which connected the northern Vienna Basin with the lagoon of the Mistelbach Basin. As the stratification indicates a west-directed progradation of sediment bodies, a current entering the lagoon was the main controlling factor for bedform formation. The huge foresets are interpreted, therefore, as flood tidal delta foresets. During the westward migration of the delta, the steep foresets gradually buried the preceding ones. At the time of flood tidal delta growth, the relative sea-level in the Vienna Basin was quite stable (Papp, 1956), and a coinciding loss of accommodation space can therefore be predicted. This assumption is supported by the upsection changing geometry of the foresets.

Towards the top of Unit 2, the regular foreset pattern is replaced by a more wavy and partly channel-like bedding. These structures might either represent large lobate foresets or longitudinal tidal bars, as described by Lesueur *et al.* (1990) from the Miocene of the Rhone Basin. However, their internal structure is identical to that of the planar-bedded foresets. This morphological shift is interpreted to be caused by a shallowing-upward trend. Consequently, current velocity probably increased, being reflected in a succession from lower-speed bedforms towards higher-speed bedforms

Table 1. Total mollusc fauna recorded from the shell dunes, based on museum collections

Bivalvia
Modiolus subincrassatus (d'Orbigny)
Obsoletiforma obsoleta vindobonensis (Laskarev)
Obsoletiforma ghergutai (Jekelius)
Inaequicostata politioanei (Jekelius)
Plicatiforma latisulca (Münster)
Sarmatimactra eichwaldi (Laskarev)
Solen subfragilis Eichwald
Donax dentiger Eichwald
Ervilia dissita podolica Eichwald
Mytilopsis sp.
Venerupis gregarius (Partsch in Goldfuss)
Gastropoda
Acmaea soceni Jekelius
Gibbula podolicum (Dubois)
Gibbula poppelacki (Hörnes)
Gibbula picta (Eichwald)
Theodoxus crenulatus (Klein)
Hydrobia frauenfeldi (Hörnes)
Hydrobia sp.
Granulolabium bicinctum (Brocchi)
Potamides nodosoplicatum (Hörnes)
Potamides disjunctus (Sowerby)
Potamides hartbergensis (Hilber)
Cerithium rubiginosum Eichwald
Melanopsis impressa Krauss
Euspira helicina sarmatica (Papp)
Ocenebra striata (Eichwald)
Mitrella bittneri (Hörnes & Auinger)
Duplicata duplicata (Sowerby)
Acteocina lajonkaireana (Basterot)
Gyraulus vermicularis (Stoliczka)
Tropidomphalus gigas Papp
Cepaea gottschicki Wenz

(Rubin & McCullogh, 1980; Costello & Southard, 1981; Dalrymple, 1984; Terwindt & Brouwer, 1986). Despite the virtual dominance of gravel-sized shells and pebbles, the deposits are mainly composed of the sand grain-size class. Even the higher amount of gravel occasionally observed in the outcrop does not contradict an interpretation as a dune. As demonstrated by Carling (1996), the predominant sediment grain size is not a major control for dune formation in coarse sediment; 2-D and 3-D dunes may even form from coarse gravel.

At first glance the overall geometry is therefore strongly reminiscent of 2-D dunes (*sensu* Ashley, 1990) and resembles the *Class IIIA* category of tidal dunes of Allen (1980). Steep foresets with downslope angles of 20° develop beneath a large-scale separated flow. During phases of substantial slackening of currents the foresets became separated by thick mud drapes. However, interpreting the foresets as slipfaces of giant dunes would result in problematic inferences with palaeogeography, namely with the depositional depth.

Although there is considerable doubt about a straightforward correlation between dune height and flow depth (e.g. Stride, 1970; Terwindt & Brouwer, 1986; Allen & Homewood, 1984; Flemming, 2000), several authors including Allen (1980), Yalin (1972), Allen *et al.* (1985) and Mosher & Thomson (2000) have discussed a vague correlation between dune height and total water depth. Following the various rules of thumb presented by the mentioned authors, a total water depth ranging from 40-90 m would have to be calculated for the 10-13 high structures of Nexing. Based on the topographic altitude of the correlative littoral deposits of the shallower oolite shoal, this depth estimation turns out to be much too deep. Especially the marker horizon in Unit 3, suggesting a phase of emersion of the entire shoal, allows a good correlation of the deposits throughout the Mistelbach block. Hence, a maximum water depth of 10-20 m is most plausible and an interpretation as a dune field is rejected. Nevertheless, bioclastic sand dunes from Ackers Shoal (Torres Strait, NE Australia) reach a height between 3-8 m in a moderate water depth of around 20 m (Keene & Harris, 1995), and therefore an interpretation as "mega"dunes cannot be ruled out completely.

A second possibility is to discuss these structures as washover deposits that formed along the seaward fringe of the shoal. However, this contrasts with the internal architecture of the shell dunes and ripples, which points to regular short-term high-energy conditions rather than to random events. Furthermore, the steep-angled foresets differ distinctly from the subhorizontal to low-angle planar stratification as described by Schwartz (1982) from washover fan deltas.

Biofacies

The statistically important molluscan species are the same in all samples, but the predominance of single taxa varies (Fig. 10). Due to the poor sorting of the shell fragments, differences in the composition of the five samples cannot be explained solely by transport. Thus, the composition might rather reflect differences in the community structures of the source areas. The shell ripple from which sample KSN4 derives is characterized by a conspicuous predominance of hydrobiid and batillariid gastropods. Therefore, the shell concentration

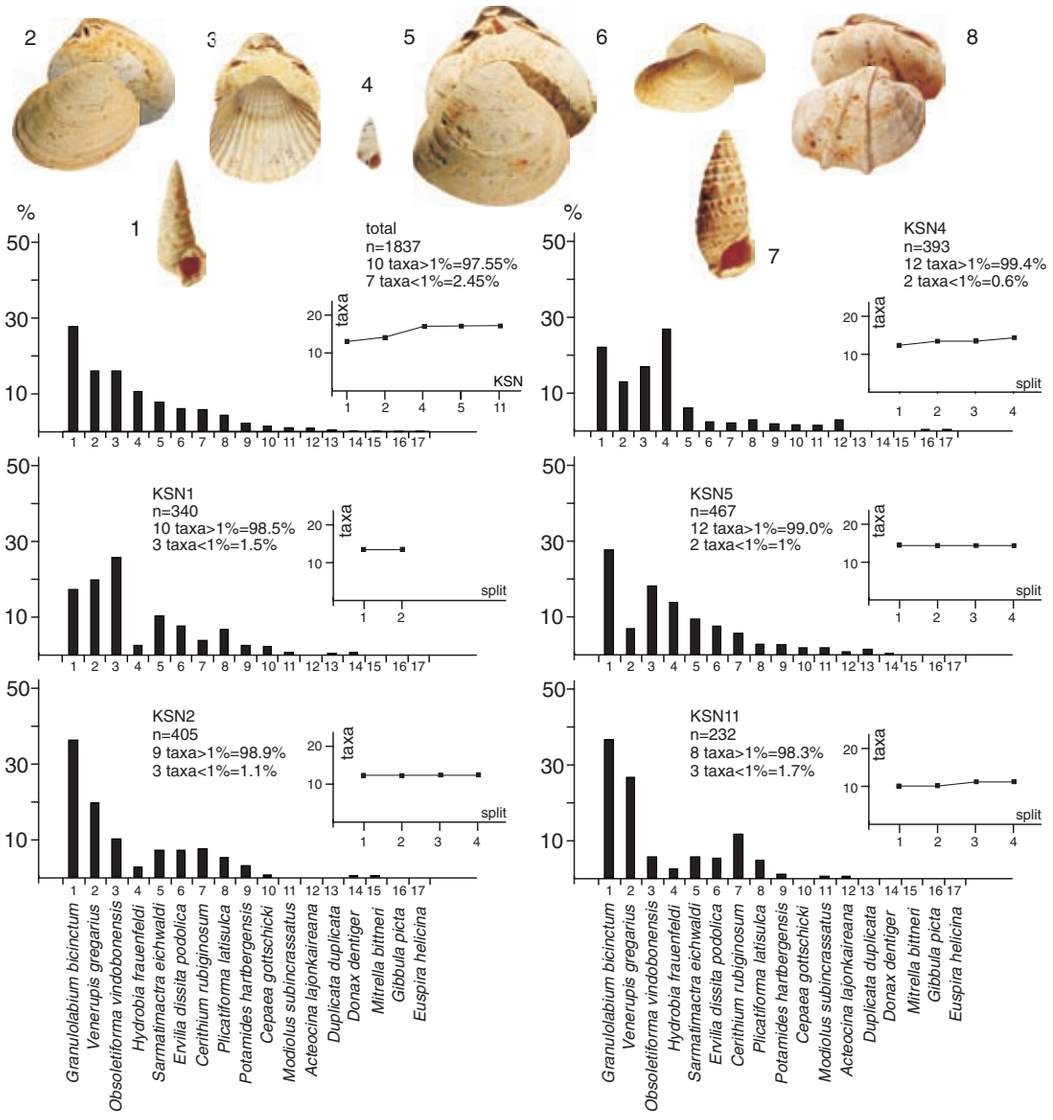

Fig. 10. Taxonomic composition and percentage abundance of mollusc species in five standardized bulk samples and for all samples (total). The eight quantitatively most important taxa are illustrated. Determination of bivalves is based on hinges and umbos; fragments are not included. Species-sampling curves for each sample (KSN1, 2, 4, 5, 11) and for all samples (total) are drawn, documenting a well-balanced sampling quality and quantity.

seems to have been fed by an intertidal environment where these taxa flourished (Latal *et al.*, 2004). In contrast, samples KSN1 and KSN2, which derive from the base of the succession, contain fewer hydrobiids but yield more foreshore and shoreface taxa such as venerid, mesodesmatid, donacid, and cardiid bivalves.

Small-sized gastropods such as the hydrobiids and *Acteocina lajonkaireana* frequently have an ooid-like coating. This points to a time-averaged accumulation of dead shells, which partly spent a long time in a wave-swept environment prior to their incorporation in the shell ripples. Most of the comparatively rare vertebrate remains also display traces of abrasion.

The supposedly high-energy environment of the shell deposits and the lack of bioturbation within the ripples as well as within the mud/sand drapes assigns these settings as an extremely unlikely natural habitat of the molluscs. Outcrops to the west and south of the Steinberg elevation document an extended area of very shallow-marine settings

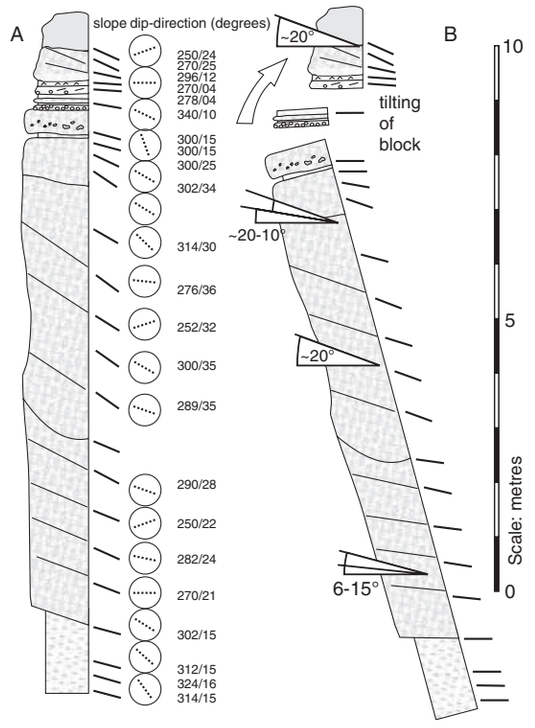

Fig. 11. Composite section for the shoal succession. (A) Idealized composite section. The dip of the foresets is consistently towards the W and NW. (B) Back-tilted log (−15°) and tectonic phase separating Unit 2 from Units 3 and 4 (see text for discussion).

characterized by oolite shoals and sand. At these localities, many of the bivalves have articulated shells, pointing to an autochthonous occurrence.

Thus, it is suggested that the molluscs are derived from these shallow-marine intertidal to shallow-subtidal environments. The process behind how the shells became transported and finally incorporated into the shell deposits remains unknown. The position of the shell beds of Nexing is, however, immediately south of the topographic high of the Steinberg. This high zone may therefore have acted (temporarily) as island or shoal along which currents transported shells and sediment southwards. At the southern end of this topographic high, a curved island spit probably developed or a tidal inlet connected with a flood-tidal delta. Functionally this topographic high acted like a barrier island (e.g. Oertel, 1985) surrounded by oolite shoals and sand flats. The mass of shells may originate from intertidal flats or shallow-subtidal areas as well as from shore erosion along and around this topographic high (island or/and shoal).

Comparable depositional systems

No modern complex shell accumulation in planar foresets, comparable to the Sarmatian example has yet been described in detail. However, similar general structures of bioclastic sand dunes with up to 95 % biogenic carbonate were reported from the Torres Strait by Keene & Harris, (1995). The cores taken in those dunes, as illustrated by Keene & Harris (1995), seem to lack internal shell ripples. The texture of the shells and fragments in the cores reveals a subhorizontal pattern. Nesting and piling are virtually absent, pointing to a quite different depositional environment. Modern dunes of the German Bight described by Lüders (1929) display some similarities in composition. These dunes are similar in their dominance of cardiid, venerid and mytilid bivalves, but differ considerably in their internal organization. The shell accumulation there is caused by winnowing in the crest area, whilst growth results from avalanching along the lee side.

A slightly reminiscent fossil example was described by Portell *et al.* (1995) from the Pleistocene Leisey shell pits in Florida. There, the so-called upper shell bed (Fort Thompson Formation) is characterized by a high percentage of mollusc shells along with fine-grained quartz sand comparable to the deposits in Austria. Abraded shells and fragments are common and Portell *et al.* (1995) interpreted the depositional environment among other variants as a tidal channel or inlet. Details concerning the geometry and internal architecture of the sedimentary body are missing.

A lack of comparative information makes it difficult to interpret the complex internal composition of the shell dunes and shell ripples in "standard" terms of hydrodynamics. The unimodal and bimodal grain-size distributions detected in the shell ripple samples (Fig. 9) are reminiscent of grain-size distributions recorded by Allen & Homewood (1984) from a Lower Miocene tidal dune in the Swiss Molasse. In that key study, bimodal distributions occurred during the neap tides and at the transition towards the spring tides, whilst unimodal distributions developed during the spring tides. A corresponding trigger might have caused the grain-size distributions of the shell ripples. Indeed, the bimodal patterns of samples KSN3-5 were detected in a ripple that developed within a thick fine sand drape that points to low current energy.

In the following, a model will be presented for the internal structure of the flood-tidal delta

foresets, the superimposed shell dunes, and the ripples, but this has to remain hypothetical because of the lack of a modern analogue for these deposits. It is proposed that the shell ripple bedform (Type 3) might be equivalent to a sand dune foreset of Allen & Homewood (1984). This interpretation is supported by the aforementioned grain-size distributions. The intervening and sometimes eroded shell-hash layer separating the shell ripples would thus have formed during the weaker ebb flow. Consequently, the sum of ripples constituting a shell dune represents tidal bundles that formed during one major cycle. This cycle might well correspond to a spring-neap cycle. The separating fine sand drapes developing during phases of low current energy would thus coincide with neap-tide deposition. The formation of the thick sand drapes separating the superior foresets of the flood-tidal delta is thus triggered by a higher-order cyclicity which cannot be predicted within this scheme. The slacking might be seasonally induced, e.g. by storm seasons.

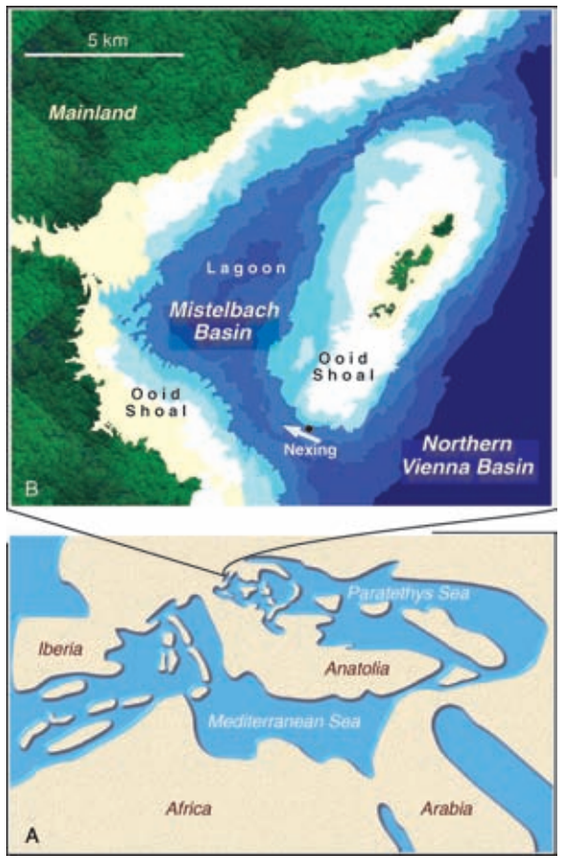

Fig. 12. Palaeogeographic setting. (A) Palaeogeography of Eurasia during the Serravallian, modified from Rögl (1998). The Paratethys Sea is nearly completely disconnected from the Mediterranean Sea. (B) The Mistelbach block during the Late Sarmatian (*Ervilia* Zone) based on sedimentological, palaeontological and tectonic information in Friedl (1936), Grill (1988), Kröll & Wessely (1993), and Harzhauser & Piller (2004a, b). The Steinberg elevation acted as an island with attached shoal about 15 km off the coast. The arrow illustrates the dominant flow direction interpreted from the foresets and subaqueous dunes at Nexing.

Palaeogeographic setting of the mollusc-carbonate factory

The palaeogeography illustrated in Fig. 12 shows that the deposits formed at the seaward margin of an oolite shoal. In the northeast of the Nexing area, the Steinberg elevation was an island whereas in the west, there was the mainland formed the coast. The island situation is reflected in by rocky littoral deposits, such as the "Riesenkonglomerat" (giant conglomerate) along the basinward side of the Steinberg elevation (Grill, 1988). This topographic accentuation is also expressed by strongly different sedimentation rates at the distinct sides of the island. About 300 m of Sarmatian deposits on the elevated block (well Mistelbach 1) contrast with a total thickness of up to 1100 m of Sarmatian sediments in close-by basinal settings (Grill, 1988). This, and the different sediment types (marls and sandy intercalations in the basin versus mixed siliciclastic-carbonate systems on the block) document that the Mistelbach block acted as a submarine shoal during the Sarmatian, about 12 Myr ago.

Due to the current pattern, inferred from the dip-directions of the foresets, most of the terrigenous material involved in the shell dune formation could not have been derived from the mainland at the time of deposition. Its origin is rather related to reactivation and reworking of deposits that accumulated along the Steinberg elevation during the earliest Sarmatian. The source for those deposits was the Molasse Basin and the Waschberg Zone. After the retreat of the Badenian Sea from the Molasse Basin, incised valleys developed in the subsequent 3rd order lowstand systems tract encompassing the Badenian/Sarmatian boundary (Harzhauser & Piller, 2004a, b). Drainage from the Molasse Basin via the modern Zaya Valley developed and transported fluvial gravel and various siliciclastics onto the Mistelbach block. During the following Early Sarmatian transgressive systems

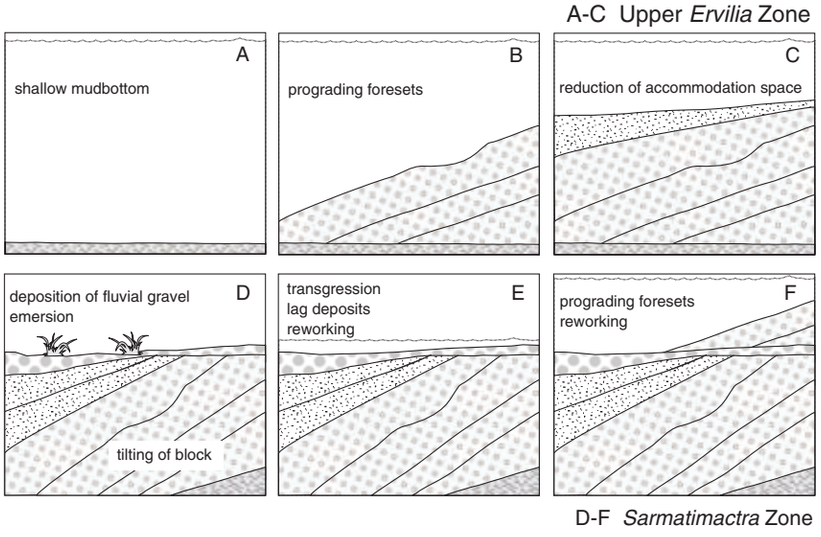

Fig. 13. Simplified evolution of the shoal on the marginal block of the Vienna Basin during the Late Sarmatian. (A-C) The growth of the flood-tidal delta started during the Late *Ervilia* Zone, with a progradation toward the west across shallow-marine clays. With successive infill of accommodation space under stable sea-level conditions, the foreset dip-angle gradually decreased. (D-F) An emergent phase of the delta, also evident in other parts of the shoal, enabled the development of vegetation. A fluvial system, transporting pebbles, spread over the dry shoal. The renewed transgression during the *Sarmatimactra* Zone led to reworking of these deposits and also allowed the re-establishment of a marine environment.

tract, the sea entered the valley and replaced the fluvial system (Papp, 1950) and the fluvial input ceased.

During the transgression, a lagoon filled the shallow Mistelbach Basin and silts were deposited in the gateway towards the deeper Vienna Basin (Fig. 13A). The shoals surrounding the Steinberg elevation, settled by enormous masses of shallow-marine molluscs, are thought to have supplied the foresets with the striking amount of shells and shell-hash. These shell masses, as well as the reworked oolites, may have been transported by SSW-directed shoal-parallel currents to the inlet where they were deposited in the prograding foresets (Fig. 13B). Thus, the WNW orientation of the downslopes of the foresets and shell dunes is interpreted to result from a dominant flood current entering the shoal via the broad inlet in the area of Nexing. In that inlet, the foresets migrated within a large channel. Similar channels with flow-transverse bedforms occur on modern oolite sand shoals of the Bahamas (Hine, 1977) and the Persian Gulf (Evans *et al.*, 1973). That channel might have been initiated during the lowstand in the earliest Sarmatian by the above-mentioned fluvial system that structured the Mistelbach block prior to the Sarmatian flooding, a mechanism frequently reported (Davis & FitzGerald, 2004).

A gradual decrease in accommodation space coinciding with the westward migration of the delta front is reflected in a shift from planar-bedded foresets towards either lobate foresets or tidal ridges (Fig. 13B and C). Finally, the shoal on which the flood-tidal delta developed became exposed during the Late Sarmatian at the boundary between the *Ervilia* Zone and the *Sarmatimactra* Zone (Fig. 13D). Fluvial gravel was deposited and vegetation developed. The subsequent flooding marking the base of the *Sarmatimactra* Zone reworked parts of the shell dunes, but also involved the fluvial gravel and oolite from the surrounding shoal (Fig. 13E). Roots that penetrated the exposed oolite caused characteristic concretions which also became reworked. Terrestrial vertebrates are most abundant in Units 3 and 4, probably as a result of lag formation and subsequent reworking. In the course of that renewed, Late Sarmatian transgression, a second flood-tidal delta developed (Fig. 13F). It, however, is strongly truncated by post-Sarmatian erosion.

CONCLUSIONS

Mollusc shells are rarely rock-forming constituents of Miocene subtropical shallow-water carbonate

factories. In the example described herein, shells of bivalves and gastropods produce large foresets of up to 13 m height with complex internal structures. The consistent dip direction to the W and WNW towards the palaeoshore suggests the flood current as the dominant flow that produced the large-scale foresets and dunes. The weaker counter current cannot be definitively detected in the sedimentary record. The planar-bedded shell-hash separating single shell ripples could be related with that weaker counter flow.

Each large-scale foreset is internally structured by two smaller bedform types. The smallest one is referred to as a *shell ripple,* attaining about 10 cm in height and up to 190 cm in length. A bundle of such ripples constitutes *shell dunes* of up to 1 m height and several metres length. If these structures escaped erosion, a thin layer of sand or shell-hash separates the dunes, being equivalents of the mud drapes of classical sand dunes. The internal texture of single shell ripples indicates that growth was a function of piling and amalgamation of shells into the direction of the dominant current. Thus, the stoss within the ripple gradually steepened. This scenario points to a prevalence of stoss-oriented growth instead of avalanching along the slipface.

The deposits described are an example of the importance of molluscs as part of Miocene subtropical shallow-water carbonate factories. However, the dominance of molluscs evolved within a unique system in which corals and coralline algae were absent due to palaeo(bio)geographic and adverse environmental factors. Instead, molluscs and ooids provided the carbonate, contributing up to 81 % of the dune sediment. Only a very small number of 5–7 mollusc species predominate in the spectrum, representing up to 98 % of the shells.

The unusual accumulation of shelly material with a relatively depleted fauna is most probably a result of the Sarmatian ecosystem that allowed only a small number of specialists to flourish. Hence, high productivity coupled with low diversity seems to support the formation of such shelly deposits. Consequently, mollusc-based carbonate factories and noteworthy shell-accumulations seem to be unusual in normal marine settings with diverse faunas. Aside from that biotic prerequisite, such shell-accumulations are linked to hydrodynamically favourable positions such as tidal inlets and channels providing suitable flow conditions for the transport of the shells.

ACKNOWLEDGEMENTS

We are greatly indebted to Bernhard Krainer and Hanns-Peter Schmid (OMV) for providing access to well log data of the Vienna Basin. Many thanks to Gerhard Niedermayr (NHMW) for the chemical analyses of the carbonate concretions and to Gudrun Höck (NHMW) and Ortwin Schultz (NHMW) for help with the vertebrates. Gerhard Penz (Vienna) kindly provided information on the mollusc fauna. The paper profited greatly by careful reviews of Giovanna Della Porta (Cardiff University), Christian Betzler (University Hamburg) and anonymous reviewers. This work was supported by the Fonds zur Förderung der wissenschaftlichen Forschung in Österreich (FWF, grants P-13745-Bio and P-14366-Bio).

REFERENCES

Abreu, V.S. and **Haddad, G.A.** (1998) Glacioeustatic Fluctuations: The Mechanism linking stable isotope events and sequence stratigraphy from the Early Oligocene to Middle Miocene. In: *Mesozoic and Cenozoic Sequence Stratigraphy of European Basins* (Eds C.-P. Graciansky, J. Hardenbol, T. Jacquin and P.R. Vail). *SEPM Spec. Publ.*, **60**, 245–259.

Allen, J.R.L. (1980) Sand waves: a model of origin and internal structure. *Sed. Geol.*, **26**, 281–328.

Allen, Ph.A. and **Homewood, P.** (1984) Evolution and mechanics of a Miocene tidal sandwave. *Sedimentology*, **31**, 63–81.

Allen, Ph.A., **Mange-Rajetzky, M.**, **Matter, A.** and **Homewood, P.** (1985) Dynamic palaeogeography of the open Burdigalian seaway. Swiss Molasse basin. *Eclogae Geol. Helv.*, **78**, 351–381.

Ashley, G.M. (1990) Classification of large-scale subaqueous bedforms: a new look at an old problem. *J. Sed. Petrol.*, **60**, 160–172.

Boersma, J.R. and **Terwindt, J.H.J.** (1981) Neap-spring tide sequences of intertidal shoal deposits in a mesotidal estuary. *Sedimentology*, **28**, 151–170.

Carling, P.A. (1996) Morphology, sedimentology and paleohydraulic significance of large gravel dunes, Altai Mountains. Siberia. *Sedimentology*, **43**, 647–664.

Costello, W.R. and **Southard, J.B.** (1981) Flume experiments on lower flow regime bed forms in coarse sand. *J. Sed. Petrol.*, **51**, 849–864.

Dalrymple, R.W. (1984) Morphology and internal structure of sandwaves in the Bay of Fundy. *Sedimentology*, **31**, 365–382.

Davis, R.A. Jr. and **FitzGerald, D.M.** (2004) Beaches and Coasts. Blackwell Science, Oxford, 419 pp.

Evans, G., **Murray, J.W.**, **Biggs, H.E.J.**, **Bate, R.** and **Bush, P. R.** (1973) The oceanography, ecology, sedimentology and geomorphology of parts of the Trucial Coast barrier island complex, Persian Gulf. In: *The Persian Gulf: Holocene Carbonate Sedimentation and Diagenesis in*

a Shallow Epicontinental Sea (Ed. B.H. Purser), pp. 233–277. *Springer*, Berlin.

Flemming, B.W. (2000) The role of grain size, water depth and flow velocity as scaling factors controlling the size of subaqueous dunes. In: *Marine Sandwave Dynamics, International Workshop, March 23-24, 2000* (Eds A. Trentesaux and T. Garlan), pp. 131–142. University of Lille 1, France.

Folk, R.L. and **Ward, W.** (1957) Brazos River bar: a study in the significance of grain size parameters. *J. Sed. Petrol.*, **27**, 3–26.

Friedl, K. (1936) Der Steinberg-Dom bei Zistersdorf und sein Ölfeld. *Mitt. Geol. Ges. Wien*, **29**, 21–290.

Galloway, W.E. and **Hobday, D.K.** (1996) *Terrigeneous Clastic Depositional Systems.* 2nd Edn. Springer, Berlin, 489 pp.

Grill, R.(1968) *Erläuterungen zur Geologischen Karte des nordöstlichen Weinviertels und zu Blatt Gänserndorf. Flyschausläufer, Waschbergzone mit angrenzenden Teilen der flachlagernden Molasse, Korneuburger Becken, Inneralpines Wiener Becken nördlich der Donau*. Geologische Bundesanstalt, Wien, 155 pp.

Harzhauser, M. and **Piller, W.E.** (2004a) Integrated Stratigraphy of the Sarmatian (Upper Middle Miocene) in the western Central Paratethys. *Stratigraphy*, **1**, 65–86.

Harzhauser, M. and **Piller, W.E.** (2004b) The Early Sarmatian – hidden seesaw changes. *Cour. Forsch.-Inst. Senckenb*, **246**, 89–112.

Hine, A.C. (1977) Lily Bank. *Bahamas: History of an active oolite sand shoal. J. Sed. Petrol.*, **47**, 1554–1581.

James, N.P. (1997) The cool-water carbonate depositional realm. In: *Cool-water Carbonates* (Eds N.P. James and J.A.D. Clarke). *SEPM Spec. Publ.*, **56**, 1–20.

Keene, J.B. and **Harris, P.T.** (1995) Submarine cementation in tide-generated bioclastic sand dunes: epicontinental seaway, Torres Strait, north-east Australia. In: *Tidal Signatures in Modern and Ancient Sediments* (Eds B. W. Flemming and A. Bartholomä). *Int Assoc. Sedimentol. Spec. Publ.*, **24**, 225–236.

Kröll, A. and **Wessely, G.** (1993) Wiener Becken und angrenzende Gebiete. Strukturkarte-Basis der tertiären Beckenfüllung. *Geologische Themenkarten der Republik Österreich 1:200.000.* Geologische Bundesanstalt Wien.

Latal, C., **Piller, W.E.** and **Harzhauser, M.** (2004) Paleoenvironmental Reconstruction by stable isotopes of Middle Miocene Gastropods of the Central Paratethys. *Palaeogeogr, Palaeoclimatol. Palaeoecol.*, **211**, 157–169.

Leclair, S.F. (2002) Preservation of cross-strata due to the migration of subaqueous dunes: an experimental investigation. *Sedimentology*, **49**, 1157–1180.

Lesueur, J.-P., **Rubino, J.-L.** and **Giraudmaillet, M.** (1990) Organisation et structures internes des dépots tidaux du Miocène rhodanien. *Bull. Soc. Géol. Fr.*, **6**, **1**, 49–65.

Lüders, K. (1929) Entstehung und Aufbau von Großrücken mit Schillbedeckung in Flut- bzw. *Ebbetrichtern der Außenjade. Senckenbergiana*, **11**, 123–142.

Mosher, D.C. and **Thomson, R.E.** (2000) Massive submarine sand dunes in the eastern Juan de Fuca Strait, British Columbia. In: *Marine Sandwave Dynamics, International Workshop, March 23-24, 2000* (Eds A. Trentesaux and T. Garlan), pp. 131–142. University of Lille 1, France.

Oertel, G.F. (1985) The barrier island system. *Mar. Geol.*, **63**, 1–18.

Papp, A. (1950) Das Sarmat von Hollabrunn. *Verh. Geol. Bundesanst.*, **1948**, 110–112.

Papp, A. (1956) Fazies und Gliederung des Sarmats im Wiener Becken. *Mitt. Geol. Ges. Wien*, **47**, 1–97.

Papp, A. and **Steininger, F.** (1974) Holostratotypus Nexing N.Ö. In: *M5. Sarmatien* (Eds A. Papp, F. Marinescu and J. Senes), *Chronostratigr. Neostratotyp.*, **4**, 162–166.

Piller, W.E. and **Harzhauser, M.** (2005) The Myth of the Brackish Sarmatian Sea. *Terra Nova*, **17**, 450–455.

Portell, R.W., **Schindler, K.S.** and **Nicol, D.** (1995) Biostratigraphy and Paleoecology of the Pleistocene invertbrates from the Leisey shell pits, Hillsborough County. *Florida. Bull. Florida Mus. Nat. Hist.*, **37**, 127–164.

Rögl, F. (1998) Palaeogeographic Considerations for Mediterranean and Paratethys Seaways (Oligocene to Miocene). *Ann. Naturhist. Mus. Wien*, **99A**, 279–310.

Rubin, D.M. and **McCullogh, D.S.** (1980) Single and superimposed bedforms of San Francisco Bay and flume observations. *Sed. Geol.*, **26**, 207–231.

Schwartz, R.K. (1982) Bedform and stratification characteristics of some modern small-scale washover sand bodies. *Sedimentology*, **29**, 835–849.

Stride, A.H. (1970) Shape and size trends for sandwaves in a depositional zone of the North Sea. *Geol. Mag.*, **107**, 469–477.

Terwindt, J.H.J. and **Brouwer, M.J.N.** (1986) The behaviour of intertidal sandwaves during neap-spring tide cycles and the relevance for palaeoflow reconstructions. *Sedimentology*, **33**, 1–31.

Yalin, M.S. (1972) *Mechanics of Sediment Transport.* Pergamon Press Oxford 290 pp..

Wessely, G. (1988) Structure and Development of the Vienna Basin in Austria. In: *The Pannonian System: A study in Basin Evolution* (Eds L.H. Royden and F. Horvath). *AAPG Mem.*, **45**, 333–346.